SAPPHIRE STATISTICAL STRENGTH FROM LASER THERMAL FRACTURE FOR SEEKER WINDOW PERFORMANCE ASSESSMENT

D. H. Platus, O. Esquivel, J. D. Barrie and P. D. Chaffee
The Aerospace Corporation, El Segundo, California

Abstract

As part of the BMDO-funded Sapphire Statistical Characterization and Risk Reduction (SSCARR) program, thin circular disks of seeker window-grade sapphire are thermally fractured using a CO_2 laser. The resulting test data will be used to benchmark window failure models being developed under SSCARR that will utilize mechanical bend-bar data obtained for sapphire with the same processing and pedigree. A significant advantage of thermal stress testing over mechanical strength testing is the avoidance of contact stresses. This is particularly important for sapphire, which is susceptible to load-point stress concentrations that can induce twinning and premature failure from rhombohedral shear. The susceptibility to twin formation and rhombohedral shear fracture in the absence of contact loads is an important question being investigated as part of this effort. The experimental test procedure and data reduction are described, and thermal fracture test results obtained to date are summarized.

Method of Approach

Laser-Induced Thermal Stresses

Biaxial tensile stresses are generated in thin sapphire disks by heating the outer annuli of the disks with a CO_2 laser, a novel method we developed at The Aerospace Corporation.[1-4] Stresses of sufficient magnitude to produce thermal stress fracture are generated near the centers of the disks, which have been optically polished to seeker window specifications. Finite element analysis (FEA) predictions of temperature profiles (and resulting stress profiles at the instant of fracture), from precisely measured time-to-failure and accurately known thermal loading conditions, are correlated with temperature vs. time histories measured with thermocouples and with LWIR thermography. A statistically significant number of disks will be thermally fractured to obtain Weibull correlations of fracture strength and statistical scatter (Weibull modulus). An additional data set will be obtained by heating the disks to a high initial temperature prior to laser heating to investigate the influence of biaxial tension on twin formation and rhombohedral shear strength. The presence of twinning is determined using cross-polarizers, and the failure mode is determined from fractography, where possible. Details of the test methodology and some preliminary experimental results with "off-the-shelf" c-axis sapphire disks have been published previously.[1-3] Finite element predictions of temperature and stress profiles for a laser annular-heated disk are shown in Fig. 1. Photos of a fractured sample and close-ups of the fracture site are shown in Fig. 2. Much information was derived from these preliminary results. The high-density parallel cracks in the central, tensile-stressed region of the disk are oriented in a direction that coincides with a crystal a-axis. The fracture surface shown in Fig. 2 is unmistakably the crystal rhombohedral plane, as determined by X-ray diffraction.

Rhombohedral Twinning and Shear Failure

We have shown theoretically that biaxial tension in the basal plane of c-axis sapphire produces the same shear on the three rhombohedral planes that is produced by uniaxial compression along the crystal c-axis. The c-axis compression at elevated temperatures produces intersecting twins and incipient crack formation, with a dramatic decrease in the sapphire compressive strength.[5-9] There is recent experimental evidence that the twinning is induced by stress concentrations at the load points.[10] The elevated temperature thermal stress tests address the question of the influence of contact loads. Rhombohedral shear strength at elevated temperatures is a critical, design-limiting factor in the design of sapphire windows and domes for certain missions.

Laser Test Facility

Laser Device

The laser device is a continuous-wave CO_2, electric discharge, recirculating gas laser that provides a peak power output of 3 kW. The laser produces a 2.5-in.-diam multimode beam having good spatial uniformity and temporal stability, with a nominal wavelength of 10.6 μm. Laser operation is computer-controlled, which allows power ramping and stabilization entirely through software command. The laser beam is directed into a Bemco chamber using gold-coated copper steering
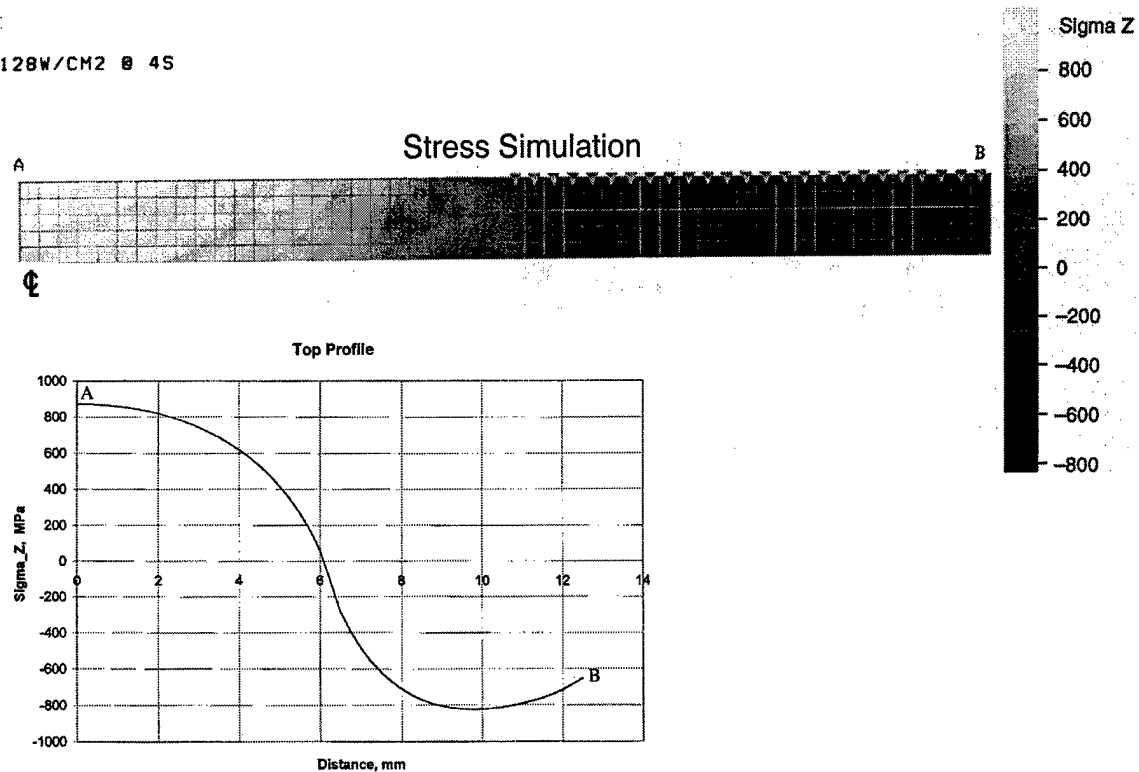
19981110 045
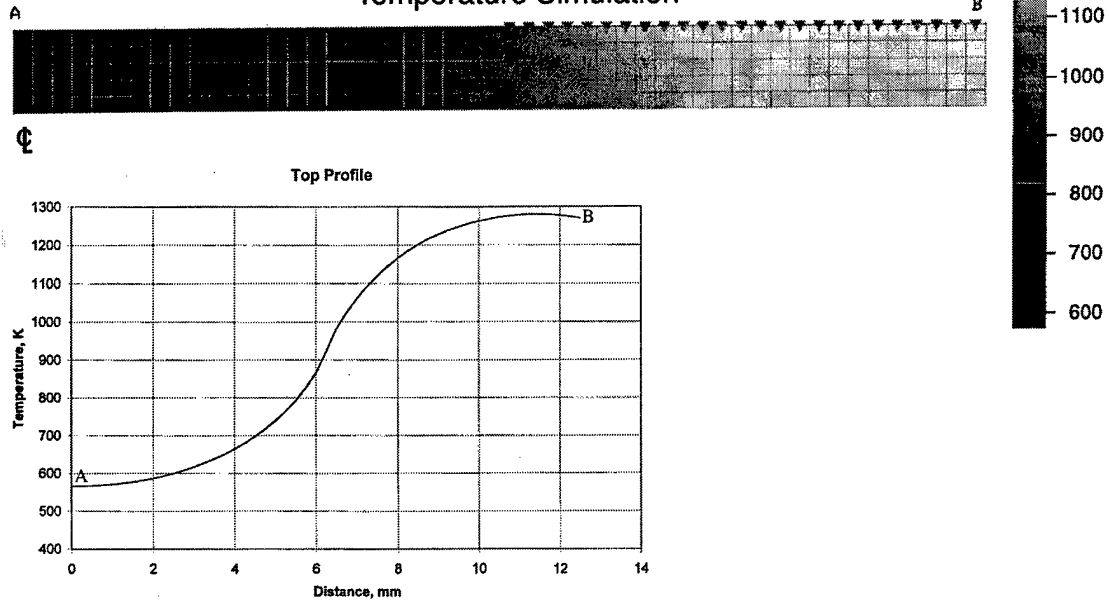
Fig. 1. FEA predictions of temperature and stress profiles for a laser annular-heated disk.
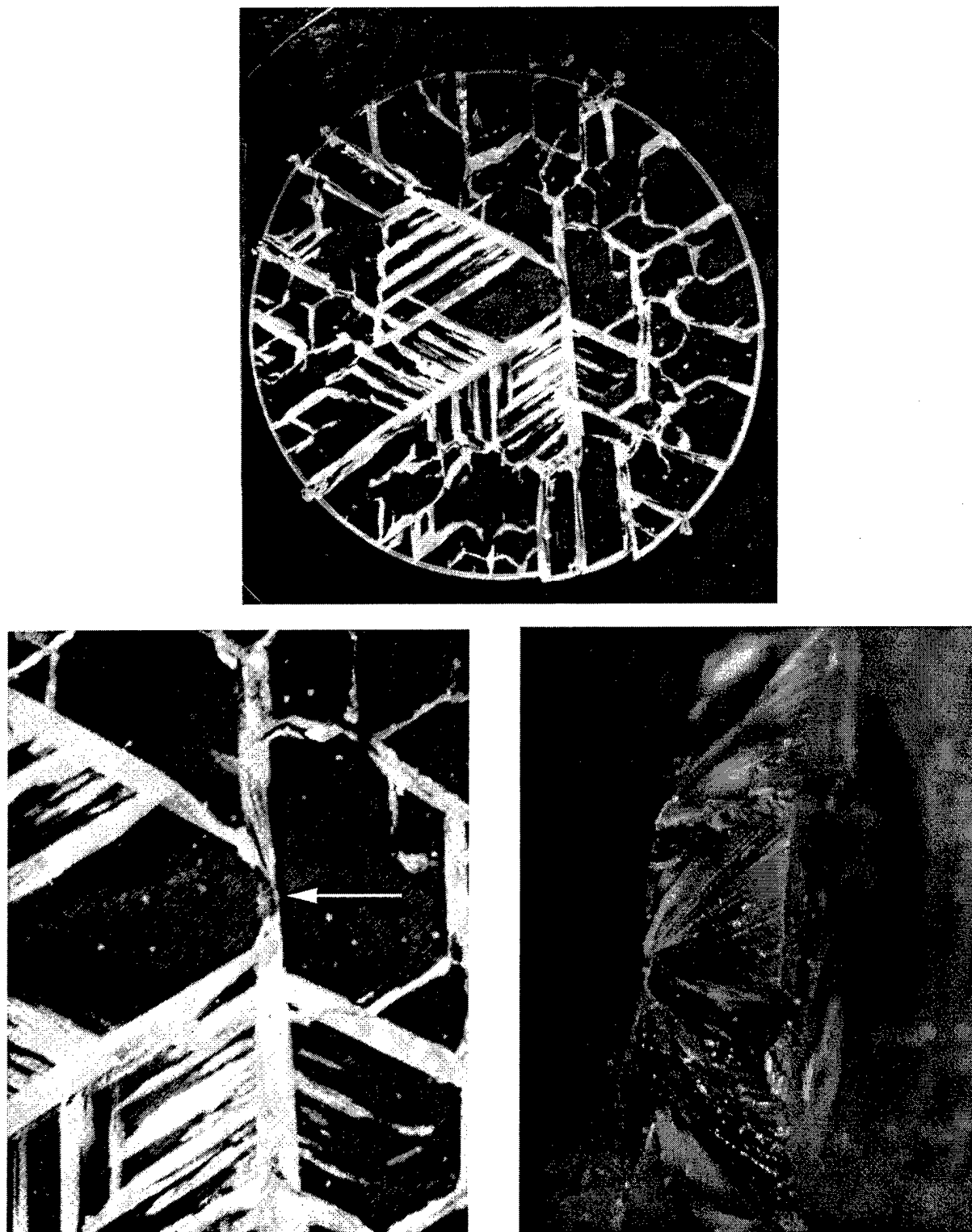
Fig. 2. Fractured disk and close-ups of the fracture initiation site and fracture surface.

mirrors, which provides for testing in vacuo if required. The SSCARR testing is conducted at ambient conditions. The beam is focused through a NaCl lens to a 2-cm-wide, 30-ms fast-acting shutter, then taken through an aperture to a turning mirror and directed through another circular aperture that is slightly larger than the sapphire disk.

Sample Holder and Instrumentation

Schematics of the disk sample holder and heating element for the elevated temperature tests are shown in Figs. 3 and 4. A thin circular platinum foil reflector is aligned at the center of the disk; this defines the outer
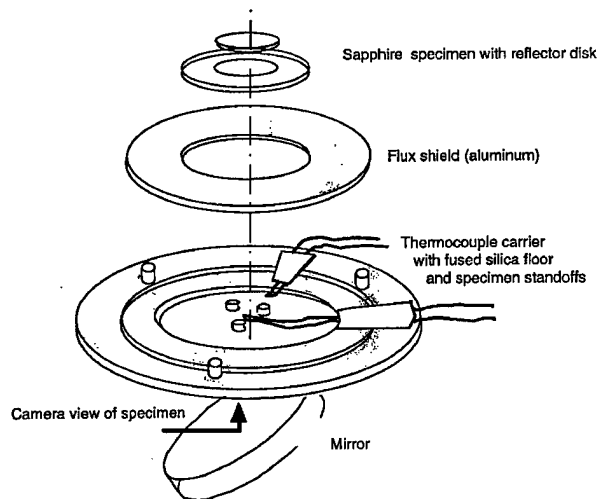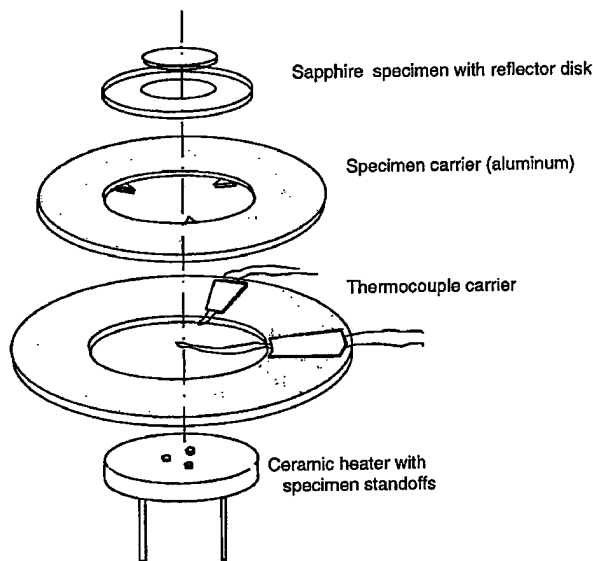
annular region of laser heating. A piezoelectric acoustic emission transducer is used to detect the instant of thermal fracture and to trip the fast-acting shutter to terminate laser exposure, thereby providing an accurate measure of the exposure time duration from shutter opening to crack detection. The laser power delivered to the sample and the power density distribution are accurately measured with a laser power meter and with LWIR imaging. This is accomplished with the use of a beam splitter, which diverts a small fraction of the total laser output along the optics train and through the circular aperture at the target location. Computerized LWIR images characterizing the spatial distribution of power in the beam are shown in Fig. 5. Two orthogonal cuts and 3-D representation using a reduced data set are presented to illustrate beam uniformity. With the laser operating at 1 kW, variations in spatial power density are within ±2 to 3%. At 2 kW power, the spatial variations are approximately twice these values. The temperature of the laser-heated surface is monitored using an infrared (IR) camera (Inframetrics 600) and stored on videotape. This IR camera normally operates by sensing emitted thermal radiation in the 8 to 14 μm wavelength band. An 8–9.5 μm bandpass filter is used to eliminate false thermal effects from scattered 10.6 μm laser radiation. A hotplate-heated sapphire coupon is used to calibrate the IR camera readings with a surface-mounted thermocouple prior to testing. The disk back-face centerline temperature and edge temperature behind the heated annular region are measured with thin-foil thermocouples.
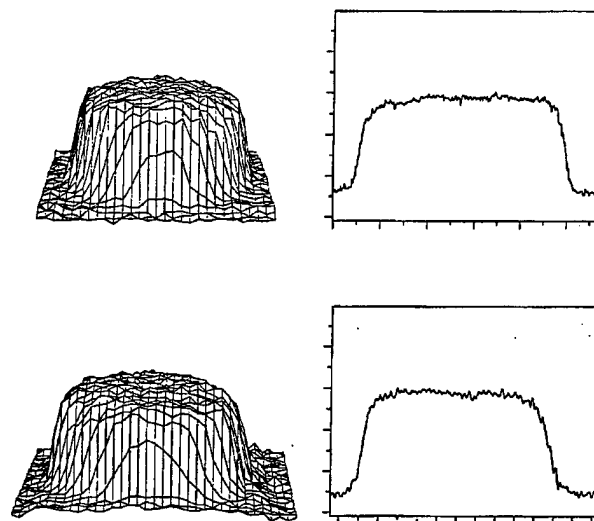

Fig. 3. Disk specimen set-up schematic..

Fig. 4.   Disk specimen set-up schematic with heating element.

Fig. 5.   Computerized LWIR images of beam power spatial distribution.

4

Data Acquisition and Control System

The laser heating cycle and data collection are computer-controlled using a LabVIEW-based interface control program designed for these experiments. After stabilizing laser power for the desired level of target heat flux, the shutter is opened. This command triggers the acquisition of a multichannel, high-rate data stream (1000 points per second) containing time, thermocouple temperatures, and fracture signals. The acoustic emission transducer is sufficiently sensitive to provide a distinct signature of the fracture event, which, with the shutter activation signal, provides time-to-failure data with an accuracy of about 0.5–1.0 ms. The fracture acoustic signal also triggers a relay circuit that closes the laser shutter within 0.5 ms of fracture. This prevents overheating of the fractured sample and provides a reasonably close event marker from which to correlate the fracture time on the videotaped IR imagery.

Test Results

Test Cases

Nine pathfinder test cases conducted to date are summarized in Table 1. The disk samples are Crystal Systems, c-axis, single-crystal sapphire. The pathfinder tests were conducted with different laser heating rates and with different locations of the outboard thermocouple. Included in Table 1 are the initial temperature (K), the net heat flux (W/cm^2), the exposure time without failure, or time to failure(s), and the location of the outboard thermocouple.

Case 5 is a re-exposure to failure of the Case 4 disk; Case 6 is a re-exposure to failure of the Case 3 disk; Case 8 is a re-exposure of the Case 1 disk; and Case 9 is a third exposure, without failure, of the same Case 1 disk. These results are significant with regard to the question of strength degradation from thermal cycling that would result from proof testing a window for flight qualification, discussed later.

Thermal Modeling and Correlation With Measurements

Unlike conventional mechanical strength testing in which the applied stress is statically determinate, thermally induced stresses are statically indeterminate and must be derived from thermostructural modeling. This requires a precise description of the sample thermal load environment and accurate thermophysical and mechanical properties from which to predict the stress state at fracture using FEA. The principal measurement diagnostics used to validate the FEA predictions are surface temperatures derived from thin-foil thermocouples. The thermocouples are located on the back surface of the disk, one at the disk center and one behind the annular, laser-heated region of the disk. Temperature-time histories derived from the thermocouple measurements are compared with the FEA predictions in Fig. 6 for Cases 1, 5, and 6. In all cases where fracture occurs, there is a distinct perturbation in the thermocouple temperature trace that signals the instant of fracture. The time to fracture is also derived independently from the acoustic transducer signal, which gives a precise measurement of the laser exposure duration from shutter opening to crack detection.

Data Summary and Predicted Stresses

A summary of predicted maximum and minimum temperatures and resulting maximum biaxial tensile stresses at the maximum exposure time are shown in Table 2. The minimum temperature occurs at the disk centerline back surface, and the maximum temperature occurs on the front exposed surface near the outer edge (see Fig. 1, for example). The location of the maximum temperature varies slightly, depending on the laser exposure parameters and initial temperature. The maximum tensile stress occurs at the disk centerline upper surface where temperatures are near minimum. The temperature gradient through the disk thickness at the centerline is on the order of one degree.

Fractured Samples

With the exception of Case 2, which failed at the lowest stress level of the tests to date, the disks fractured into too many pieces to reconstruct the original disks. A plan view of the Case 2 fractured disk is shown in Fig. 7. The failure initiated near the disk center, as determined from a fractographic examination. By comparison with the fractured disk shown in Fig. 2, the crack pattern is much more sparse, indicating a lower level of stored strain energy at failure. The six-fold symmetry of the a-axis crack patterns in the central, tensile-stressed region of the disk is apparent in both cases. These thick radial cracks, apparent in plan view, have been verified to be projections of the rhombohedral fracture planes on the basal plane, which is the surface plane of the disk. The rhombohedral plane is oriented at 57.6° to the c-axis, such that, for the 1-mm-thick disk, the projected crack thickness is 1 mm × cot(57.6°), or 0.635 mm. No twins were observed in any of the fractured samples, including the pre-heated Case 7, which reached a measured central

Table 1. Test Cases

Case No.	Initial Temp (K)	Flux (W/cm²)	Exposure Time (s)	Outboard TC
1	RT	37	12	edge
2	RT	42	6.3 failed	edge
3	RT	41	15	edge
4	RT	53	10	0.6*radius
5 (4 rerun)	RT	78	6.8 failed	0.6*radius
6 (3 rerun)	RT	54	9.6 failed	0.75*radius
7	713	52	7.7 failed	edge
8 (1 rerun)	923	31	9.5	edge
9 (8 rerun)	923	32	13	edge

Table 2. Temperature-Stress Summary

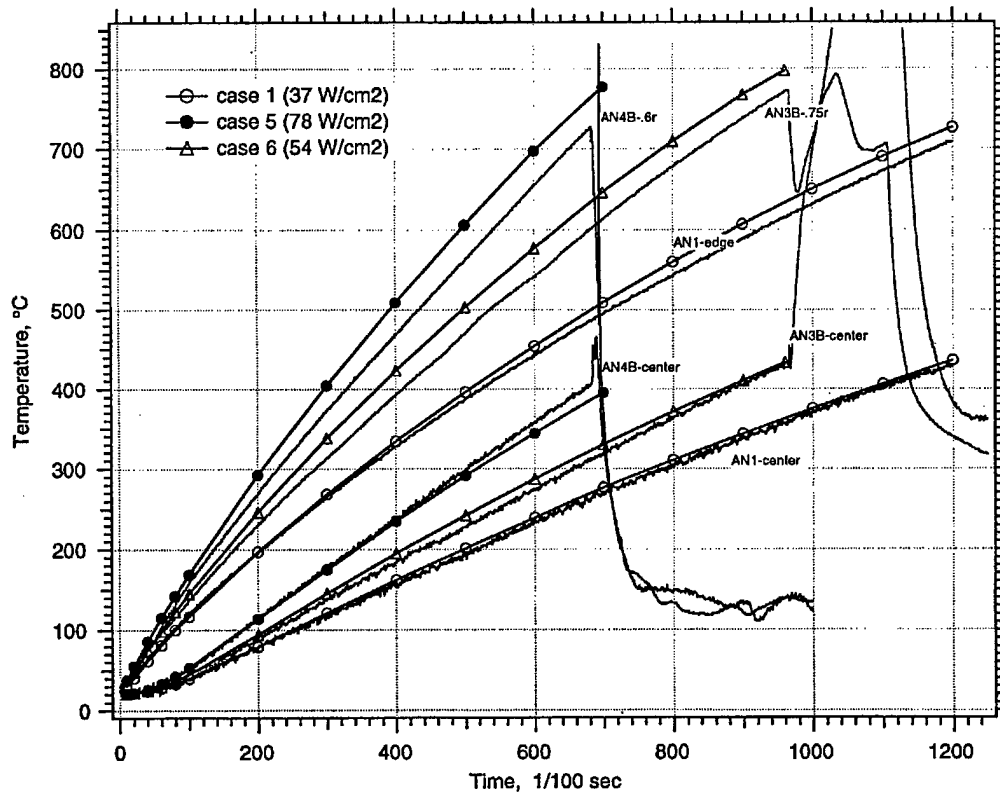| Case No.	Exposure Time (s)	Min Temp (K)	Max Temp (K)	Max Stress (MPa)
1	12	700	1006	329
2	6.3 failed	536	805	268
3	15	808	1154	385
4	10	719	1147	466
5 (4 rerun)	6.8 failed	658	1216	598
6 (3 rerun)	9.6 failed	706	1133	464
7	7.7 failed	866	1263	414
8 (1 rerun)	9.5	1017	1246	275
9 (8 rerun)	13	1067	1291	284

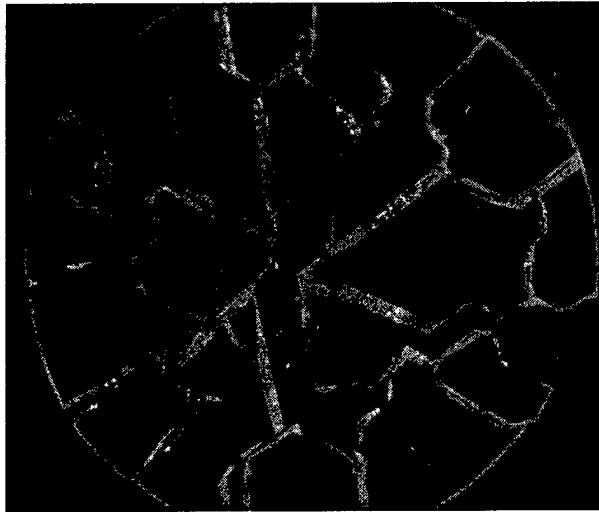Fig. 6. Comparison of predicted and measured temperature-time histories.

Fig. 7. Fractured disk.

temperature of 873K where the biaxial tensile stresses are maximum. Nor were twins observed in the pre-heated Cases 8 and 9, which reached central temperatures in excess of 1000K under peak biaxial tension.

Discussion

The dataset to date is too small from which to derive any meaningful statistics. It does appear that the strength of these SSCARR-pedigreed samples is below typical strengths measured earlier for Crystal Systems c-plane sapphire at room temperature and 500°C,[11] which bounds the range of minimum temperatures of our samples at fracture, except for the pre-heated sample. The absence of any observed twinning also suggests that the failure mode is brittle tensile fracture. This is apparently the case for the one pre-heated sample that failed near 873°C. It is noted that the fracture stress for this case is near the mean value for the four fractured samples, and is substantially higher than the uniaxial compression stress required to cause rhombohedral shear failure at 873K, as reported in Ref. 6. It is significant to note that the two samples that survived a first exposure, Cases 3 and 4, and were subsequently re-tested at a higher heat flux to failure, both failed at substantially higher stress than the level reached on first exposure. This provides some limited evidence that tends to dispel the often-raised concern that proof testing to screen out defective flight windows might damage the window through thermal cycling and reduce its strength. The proof test would be conducted at a stress level that exceeds by some margin the maximum stress expected in flight. Hence, if the window can be demonstrated to survive to an equal or higher stress level than the proof test, on re-exposure, it should be safe to fly.

Conclusions

At completion of the pathfinder test series, a minimum of 25 samples will be tested from room temperature to failure under replicate laser heating conditions to be determined from the pathfinder test results. An additional 25 samples will be pre-heated and subsequently laser tested to investigate the influence of biaxial tension on twin formation and rhombohedral shear failure. The test results will be analyzed using Weibull statistics and compared with uniaxial bend-bar data derived for sapphire with the same processing and pedigree. The objective is to provide a sapphire statistical database and methodology from which sapphire seeker window flight performance can be predicted for arbitrary window configurations over a range of flight conditions.

Acknowledgments

References

1. O. Esquivel, J. D. Barrie, P. D. Chaffee, and D. H. Platus, "Thermal Stress Induced Failure of (0001) Sapphire Using a CO_2 Laser," AIAA Paper No. 96-2340, 27th AIAA Plasmadynamics and Lasers Conference, New Orleans, LA, 17–20 June 1996.

2. D. H. Platus, O. Esquivel, J. D. Barrie, P. D. Chaffee, and M. J. Stallard, "Thermostructural Testing of Sapphire Seeker Windows Using a CO_2 Laser," *Proc, 5th Annual AIAA/BMDO Technology Readiness Conference*, Eglin AFB, Ft. Walton Beach, FL. 16–20 September 1996.

3. D. H. Platus, O. Esquivel, J. D. Barrie, P. D. Chaffee, "Sapphire Window Statistical Thermal Fracture Characterization Using a CO_2 Laser," *Proc. SPIE Windows and Dome Technologies and Materials V Conference*, Marriott World Trade Center, Orlando, FL, 21–22 April 1997.

4. D. H. Platus, O. Esquivel, J. D. Barrie, P. D. Chaffee, and M. J. Stallard, "Thermal Fracture Test Results for Laser-Heated THAAD Seeker Window Coupons," *Proc. 7th DoD Electromagnetic Win-*

dows Symposium, JHU/Applied Physics Lab., Laurel, MD, 5–7 May 1998.

5. A. H. Heuer, "Deformation Twinning in Corundum," *Philos. Mag.*, **13**, 379–393 (1966).

6. W. D. Scott and K. K. Orr, "Rhombohedral Twinning in Alumina," *J. Am. Ceram. Soc.* **66**[1], 27–32 (January 1983).

7. D. C. Harris, F. Schmid, J. J. Mecholsky, and Y. L. Tsai, "Mechanism of Mechanical Failure of Sapphire at High Temperature," *SPIE Proceedings*, **2286**, 16–28 (1994).

8. D. H. Platus and K. P. D. Lagerlöf, "Thermostructural Failure from Rhombohedral Twinning of Convectively Heated Sapphire Window Samples," *Proc. 6th DoD Electromagnetic Windows Symposium*, Huntsville, AL, 17–19 October 1995.

9. K. P. D. Lagerlöf, "Implications of Deformation Twinning on Sapphire (α-Al2O3) Window Design," *Proc. 6th DoD Electromagnetic Windows Symposium*, Huntsville, AL, 17–19 October 1995.

10. D. C. Harris, "Overview of Sapphire Mechanical Properties and Strategies for Strengthening Sapphire," *Proc. 7th DoD Electromagnetic Windows Symposium*, JHU/Applied Physics Lab., Laurel, MD, 5–7 May 1998.

11. J. W. Fischer, D. C. Harris, W. R. Compton, and N. A. Jaeger, "Strength of Sapphire as a Function of Temperature and Crystal Orientation," Naval Weapons Center Report No. NWC TM 6866, September 1990.

8